Research Article

Polyester Functionalized Graphene Composite a Typical Corrosion Inhibitor for Mild Steel in 1M H_2SO_4

PR Sivakumar*

Department of Chemistry, Adithya Institute of Technology, Coimbatore-641 104, Tamil Nadu, India

Abstract

Condensation of substituted 2,5-bis(4'-amino phenyl)-1,3,4-oxadiazole with pimelic acid resulted in the formation of a novel heterocyclic polyester with symmetrical 1, 3, 4-oxadiazole rings. This polyester's effectiveness for corrosion prevention of mild steel in 1M H2SO4 has been investigated using the weight loss method, polarisation technique, and electrochemical impedance spectroscopy. This compound's adsorption on a mild steel surface was discovered to follow the Langmuir adsorption isotherm. The inhibition effectiveness was 38.6 percent for 500ppm of polyester, according to the data. To improve inhibitory efficiency, the polymer was transformed into a composite containing functionalized graphene. In the future, the polymer/graphene composite will usher in a new phase of corrosion prevention materials. The combination (500ppm polyester + 500ppm functionalized graphene) demonstrated up to 90% inhibitory effectiveness. FT-IR spectra, scanning electron microscope-energy dispersive X-ray spectroscopy (SEM-EDS), TGA, and XRD investigations all verified the production of composites.

Keywords: PE-FG composite, FT-IR, TGA, XRD, SEM-EDS, polarization technique, surface morphology

***Correspondence**

Author: PR Sivakumar

Email: shivarashee@gmail.com

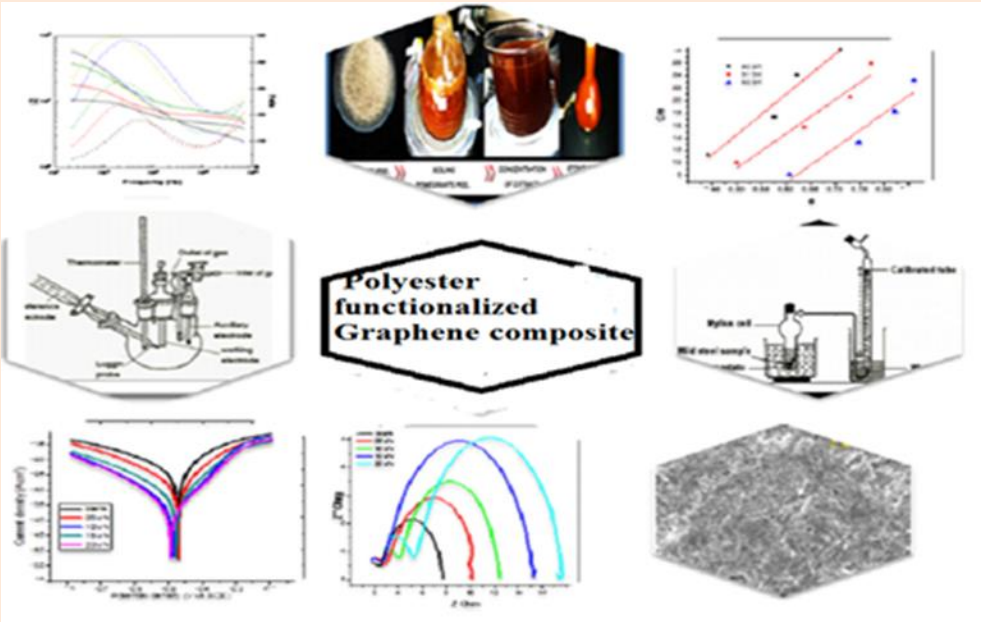

Introduction

Corrosion prevention is essential as corrosion is a very costly problem which substantially impacts the economy of the Nation [1]. Corrosion can be prevented or regulated by placing a durable protective layer of inert metals, conductive polymers [2] or thiol-based monolayers [3] between a metal and a corrosive environment, however these coatings have their limits. Several naturally occurring substance have been tried as corrosion inhibitor for mild steel in acidic medium. Most of the natural products are non-toxic, biodegradable and readily available in plenty. More investigations have been reported using naturally occurring substances (plants extract) as corrosion inhibitor for several metals in different media. The plants extracts constitute several organic compounds which have corrosion inhibiting abilities. These organic coatings inhibit ionic transport and electrical conduction, and therefore protect steel surfaces against corrosion for an extended period of time [4]. Nanofillers such as Graphene [5], TiO_2 [6, 7], SiO_2 [8,]

ZnO [9, 10], ZrO2 [11], and Fe_2O_3 [12] can increase the coatings' corrosion resistance, thermal characteristics, and mechanical properties. Graphene is chemically inert and can withstand temperatures of up to 400 degrees Celsius. Monolayer graphite is a single atom thick honeycomb lattice sheet with unique characteristics that are crucial in specialized applications. High electrical and thermal conductivity and extraordinary mechanical strength [13-14] are just a few of the many uses for this material, which can be produced on a meter-scale and mechanically transferred onto arbitrary surfaces [15]. So long as graphene sheets are clear (>90 percent transmittance for 4-layered graphene), they will not affect the optical characteristics of the underlying metal [16, 17]. There has been evidence that graphene may successfully isolate the surface from its surroundings [18-21] in recent tests. But its poor mechanical strength means it has its own set of drawbacks. To improve the corrosion resistance of the graphene/PE composite coatings in this work. Our research indicates that graphene/PE composites as anticorrosive materials have not yet been reported. The polymer composite was prepared from polyester (condensation of substituted 2,5-bis(4'-amino phenyl)-1,3,4-oxadiazole and pimelic acid) and functionalized graphene (FG) by ultra-sonication method. The efficiency of this polymer composite has been studied for corrosion inhibition of mild steel in 1M H_2SO_4 by weight loss, polarization technique, electrochemical impedance spectroscopy and atomic absorption spectroscopy. The synthesized PE and composites were characterized by fourier transform infrared spectroscopy (FT-IR), thermogravimetric analysis (TGA), wide angle X-ray diffraction spectroscopy (XRD) and scanning electron microscope – energy dispersive X-ray spectroscopy (SEM-EDS).

Experimental Method

Materials used

The mild steel specimen of size 1cm x 3cm x 0.1cm having composition 0.084% C, 0.369% Mn, 0.129% Si, 0.025% P, 0.027% S, 0.022% Cr, 0.011% Mo, 0.013% Ni and the remaining iron were used for weight loss measurements. For electrochemical methods, a mild steel rod of same composition with an exposed area of $1cm^2$ was used. The electrochemical measurements were performed in a classical three-electrode cell assembly. The potentiodynamic polarization curves were obtained from -200mV to +200mV (versus OCP) with a scan rate of 1 mV/s. The data were collected and analyzed by IVIUM software. EIS measurements were carried out at a frequency range of 10 KHz to 0.01Hz with a superimposed sine wave of amplitude 10mV. The synthesized polyester composites was confirmed by IR spectra using Shimadzu IR Affinity 1 spectrometer. In order to determine the thermal stability of the polymer and composites, TGA was carried out. The thermo grams were recorded in dynamic nitrogen atmosphere with a heating rate of 10^{o}C using a Perkin Elmer (TGS-2 model) thermal analyzer. X-ray diffractometer (XRD; Bruker D8 Advance, Germany). The surface morphology was recorded with an EDS detector coupled with SEM using Medzer biomedical research microscope (Mumbai, India).

Synthesis of polyester, FG and PE-FG composite

Synthesis of Monomer:

Stage – I

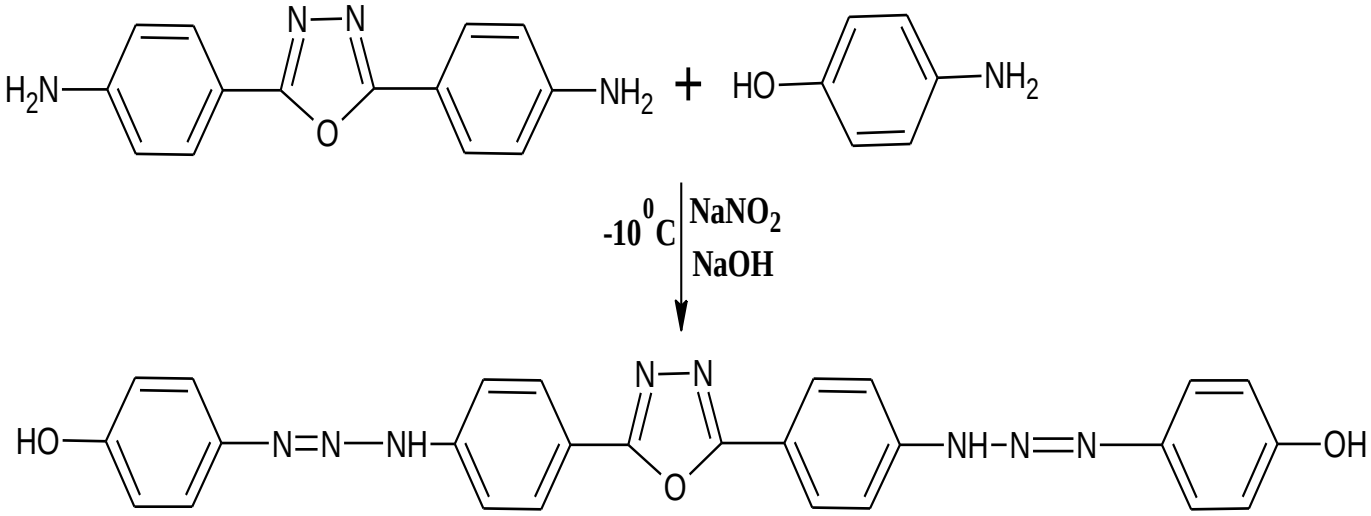

Stage: II

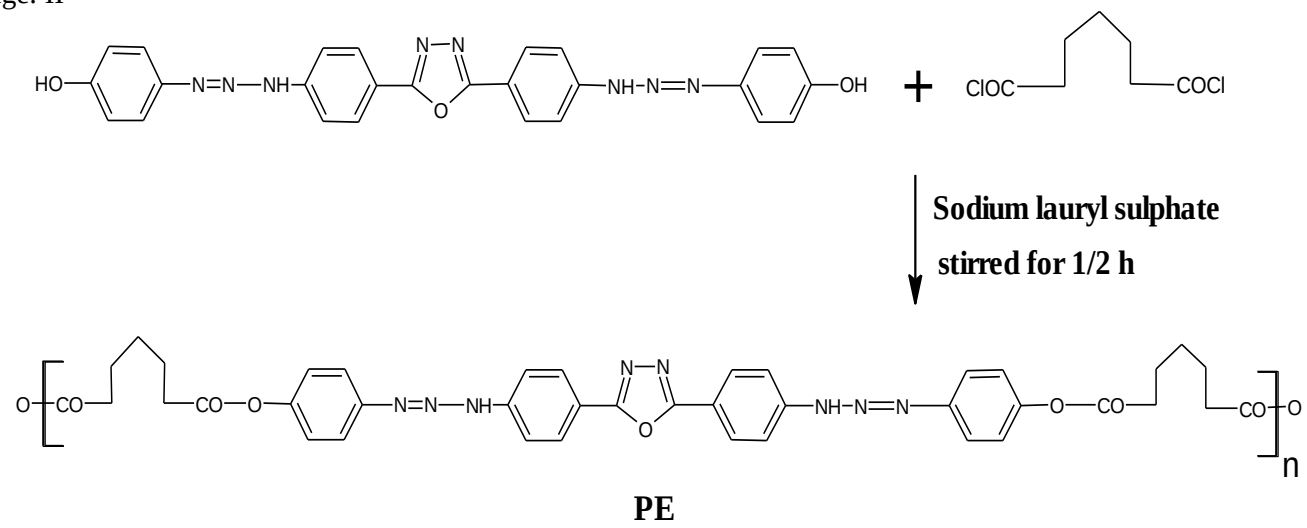

PE

Synthesis of polyester [PE]

With a little quantity [22] of PPA, p-amino benzoic acid is hydrate with hydrazine. Monomer I was dissolved in 10 percent NaOH solution with 0.01M of 2,5-bis(4-aminophenyl)-1,3,4-oxadiazole, and then the diazonium salt solution (4-amino phenol and $NaNO_2$) was added over a period of 25 minutes and the mixture was agitated for three hours. A little quantity of sodium lauryl sulphate was added to this and swirled for 30 minutes. Pimeloyl chloride was added next, followed by acetone and chloroform.

Synthesis of functionalized graphene [FG]

PPA (40g), P2O5 (20g), and 4-aminobenzoic acid (2g) were put in the resin flask, which had a high torque mechanical stirrer, nitrogen inlet valve, and exit valve. Under dry nitrogen purge conditions at 80 °C, the mixture was agitated for an hour at 80°C. This was followed by heating the reaction mixture to 100°C and stirring it for an hour. The combination was then heated to 130 C and kept at that temperature for 72 hours, according to the study. Using suction filtration, the resultant precipitate (dark brown in colour) was washed with water.

Synthesis of polymer composite

Stage: III

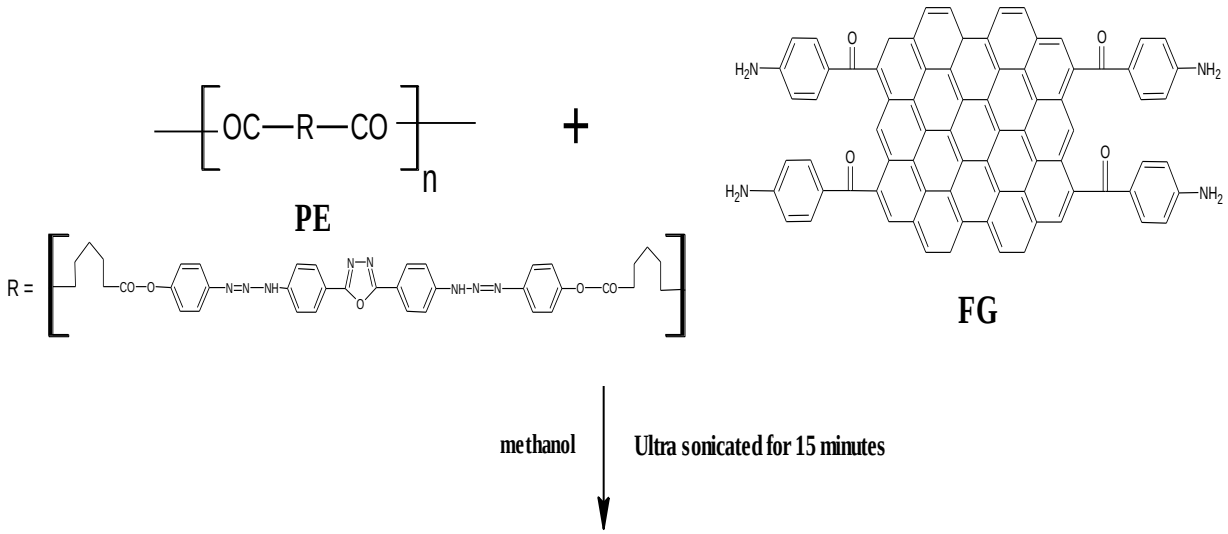

PE-FG composite

After adding 10ml of PE (500ppm), a suitable quantity of FG (100pg, 300pg, and 500ppm) was distributed into the solution using ultra sonication for 15 minutes. As an inhibitor, the ultrasonicated products were dried.

Results and Discussion

Characterization of PE, FG & PE-FG composite and corrosion studies

Infra-red spectra

To determine the existence of functional groups in organic molecules, one of the most significant techniques is FT-IR spectroscopy. **Figure 1a** shows bands at 3020 cm^{-1}, 1679 cm^{-1}, 1600 cm^{-1} and 1200 cm^{-1}, which correspond to -NH, >C=O, >C=N and C-O-C groups correspondingly in the IR spectra of PE (Figure 1b) except for the modest wide peak at 1700cm^{-1} which corresponds to aromatic C=O stretching [27]. A prominent peak can be seen at 1636.38cm^{-1}, which is indicative of the >C=O group and 3400cm^{-1}, which is diagnostic of the -NH_2 group in the FG (Figure 1c). Functionalized graphene (FG) was successfully produced as a consequence of covalently linking graphene-like sheets to 4-aminobenzoyl groups (Figure 1c). Its IR spectrum (Figure 1d) is a mixture of the PE-spectrums, FG's with bands at 3024cm^{-1},3356cm^{-1}, 1683cm^{-1}, 1543cm^{-1}, and 1203cm^{-1}, which correspond to the -NH, >C=O and C=N groups respectively. This indicated that the composite had been successfully formed and that it was stable. In Figure 1e, composite and metal surfaces were exposed to H_2SO_4 solution for 3 hours and their FT-IR spectra were blended together. Similar kind of peaks may be attributed to the spectra of the metal surface formed in the presence of polyester composite (PE-FG). Adsorption of polyester composite (PE-FG) on mild steel surface by physical forces rather than chemical combination is well demonstrated.

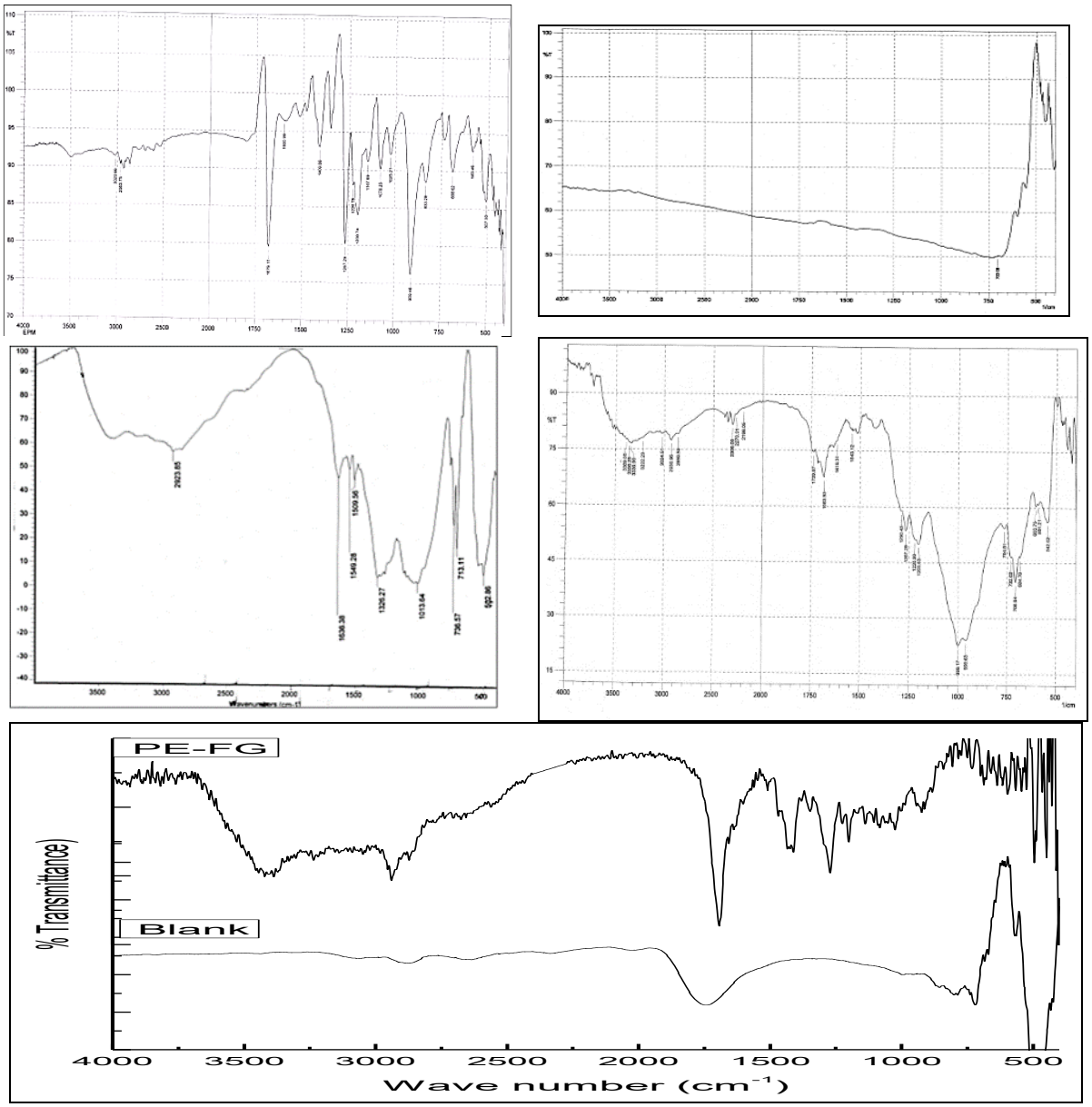

Figure 1 IR spectra of mild steel plate immersed in the presence and absence of the inhibitor in 1M H_2SO_4

Thermal analysis

Temperature gravimetric analysis (TGA) can be used to quantify the degree of functionalization, as shown in **Figure 2**. This graphite was stable in N_2 up to 900 degrees Celsius, while the graphite in the FG sample showed a weight loss of 30% around 400 degrees Celsius This early weight loss in FG is attributed to the 4-amino benzoyl moiety that was covalently attached to the edges of the graphite. The thermal degradation of PE takes place in a single step around 270-320˚C which may be attributed to the main pyrolitic rupture of –N=N-, commencing at about 300˚C with the evolution of aromatics from the degradation of the oxadiazole backbone [28]. Using a TGA, the deterioration of PE-FG composite may be seen in two stages. In the PE-FG composite, the loss of adsorbed water causes the first step at 80-130˚C. Both PE and FG are degrading around 400-450˚C. Polymer degradation has changed from 320 to 400˚C, which is a higher temperature. According to this, there is a significant contact between the polymer matrix and the FG layers, which results in a reduction in polymer mobility near the interface [28]. At 600˚C, the PE residue is 10% and the composite residue is 60%. Functionalized graphene, it appears, boosts polymer surfaces' ability to char up to 600°C by increasing the development of char on the surface of the polyester.

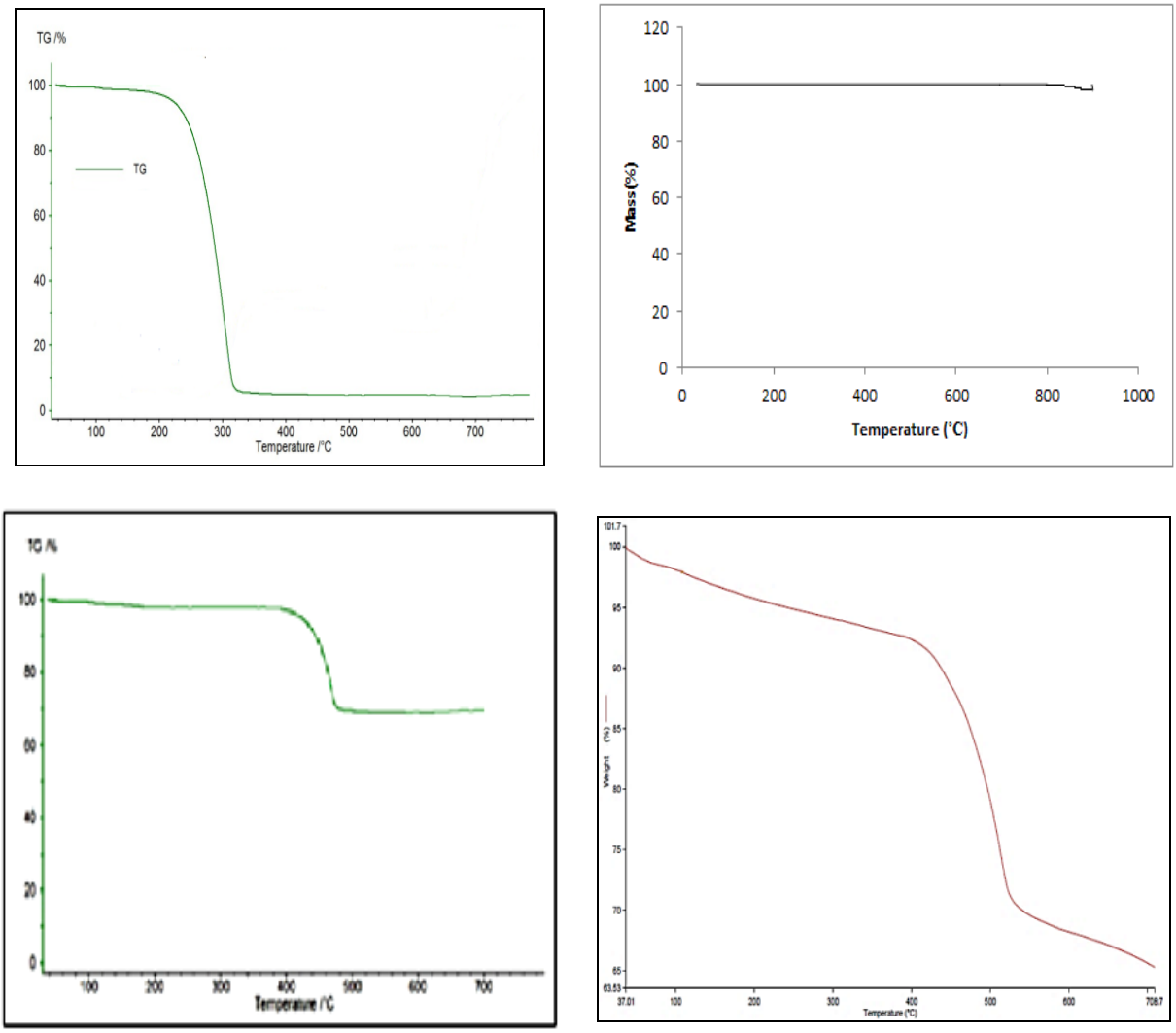

Figure 2 (a) Thermogram of PE, (b) Thermogram of graphite, (c) Thermogram of PE-FG Thermogram of FG

XRD Analysis

On the right, you can see the XRD pattern for PE-FG, which shows the mixture of both PE and FG. As a result of the delamination of graphite, the intensity of the graphitic peak at 2θ = 26.3° reduced, confirming the attachment of 4-amino benzoic acid to the edges of graphite without basal plane functionalization [29]. There are still a few peaks that match to PE which suggests that the polymer has a more crystalline structure. Hence, the existence of both PE and FG indicates that the composite PE-FG has been successfully formed. **Figure 3** shows the XRD patterns of mild steel submerged in 1M H_2SO_4 with inhibitors and without inhibitors. Disturbances in the X-ray pattern are caused by the

irregularity of the substrate's surface. There are three distinct iron peaks at 2θ = 28.2, 35.3, and 62.1 degrees in the XRD pattern of mild steel in blank solution (Figure 3 blank). Oxides of iron appear as peaks in the X-ray diffraction pattern of the polyester composite (PE-FG). Fe_3O_4 and FeOOH iron oxides are found on the surface of metals submerged in acid [39]. The intensity of the peaks owing to iron oxides is extremely low, whereas the intensity of the peaks due to iron alone is very high. This demonstrates that the polyester composite protects the mild steel surface.

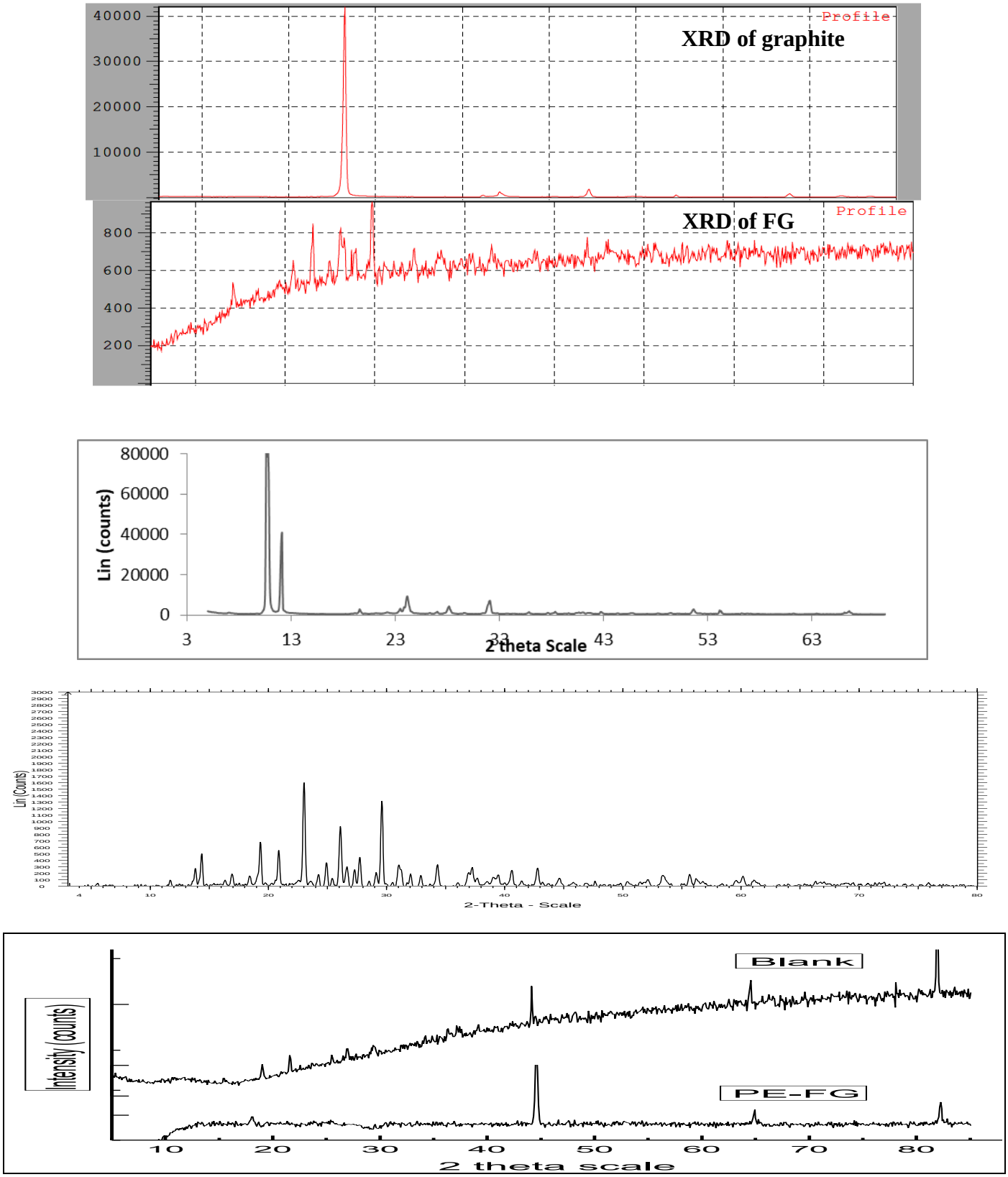

Figure 3 XRD pattern of PE –FG and mild steel surface in the presence and absence of inhibitor in 1M H_2SO_4

Scanning electron microscope-energy dispersive X-ray spectroscopy

According to SEM images, there are several intriguing morphological variations between the filler material, polymer, and polymer composite, according to the study (PE-FG). However, the porous character of the polymer and its rough surface are clearly evident from its SEM picture [30]. As illustrated in **Figure 4**, the polymer composite surface is flaky (a, b and c). Plastic composite surface morphology differs from filler material and polymer surfaces. A more organised, compact and dense structure is seen. The surface of the changed polymer composite is clearly visible in the SEM photos, indicating that the surface has undergone a gradual change. Scanning electron microscopy images of mild steel specimens submerged in blank acid (1M H_2SO_4), inhibited acid (1M H_2SO_4 + 500ppm of PE), and inhibited acid (1M H_2SO_4 + 500ppm of PE + 500ppm of FG) are presented in Figure 4, respectively. The pictures demonstrate that the mild steel was extensively corroded in 1M H_2SO_4, whereas the surface condition was much improved in the presence of inhibitor PE-FG. There may be a protective coating of inhibitor molecules adsorbing on the surface of the mild steel that decreases corrosion rates by a significant amount.

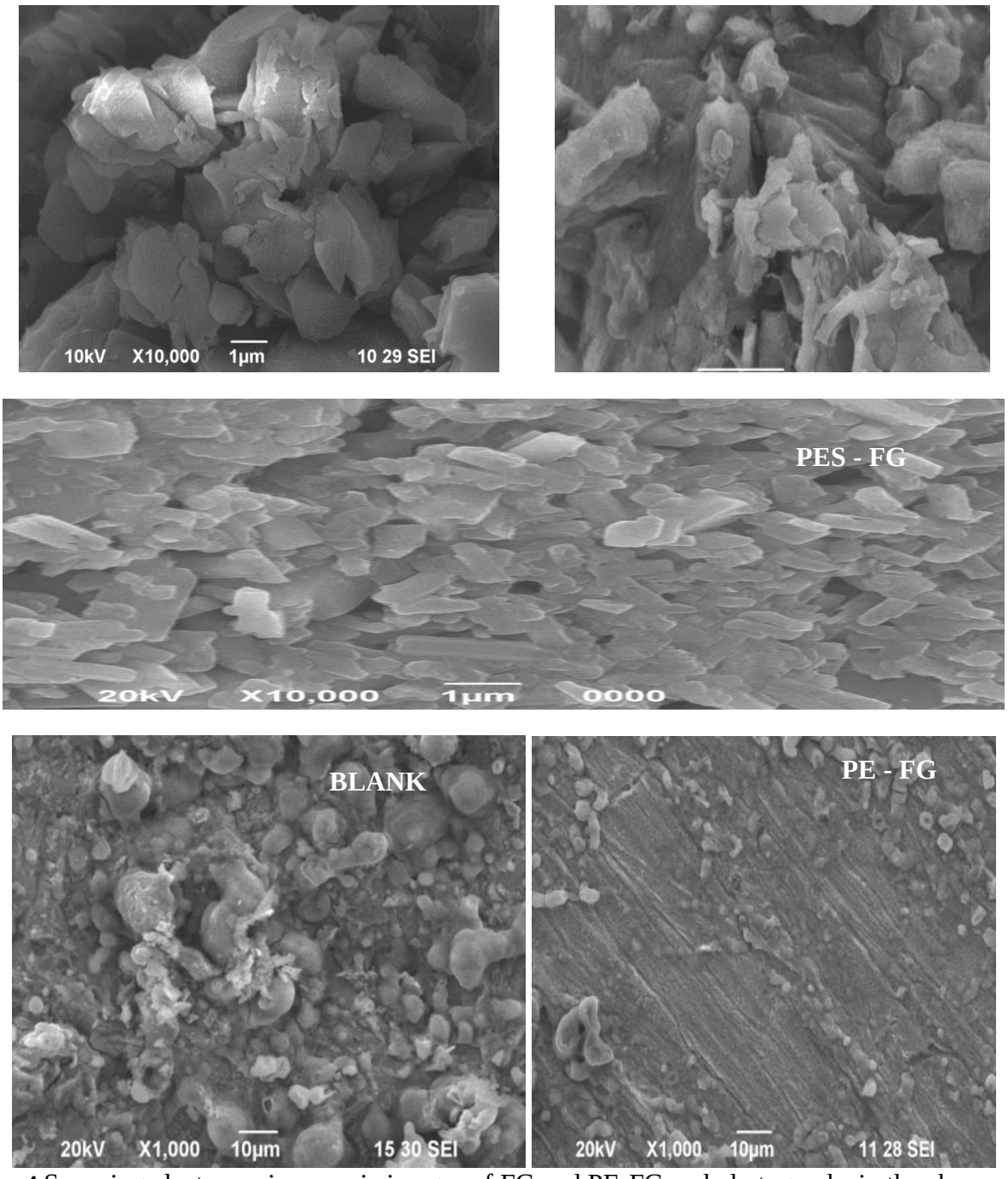

Figure 4 Scanning electron microscopic images of FG and PE-FG and photographs in the absence and presence of inhibitor

EDS of polymer composite and corrosion studies

Quantitatively, an EDS examination determines which components are present in the polyester composite. An element's concentration cannot be quantified by the intensity of the EDS peak, but relative quantities can be deduced from relative peak heights [30]. Carbon, oxygen, nitrogen, sulphur, and other elements are confirmed in the polyester composite (PES-FG) by EDS microanalysis, as shown in **Figure 5** and **Table 1**. A successful composite has been formed, as evidenced by this observation. On the mild steel samples, Figure 5 and Table 1 show the EDS spectrum and the elements' % atomic content, respectively. As shown in Figure 5a, the distinctive peaks of the components that make up mild steel are visible in absence of the inhibitor. Figure 5b shows an extra peak due to the presence of C, N, and O in the polyester composite (PES-FG). This was confirmed by the presence of C, N, and O peaks in an EDS pattern of the inhibitor adsorbing on the mild steel surface, preventing it from corroding.

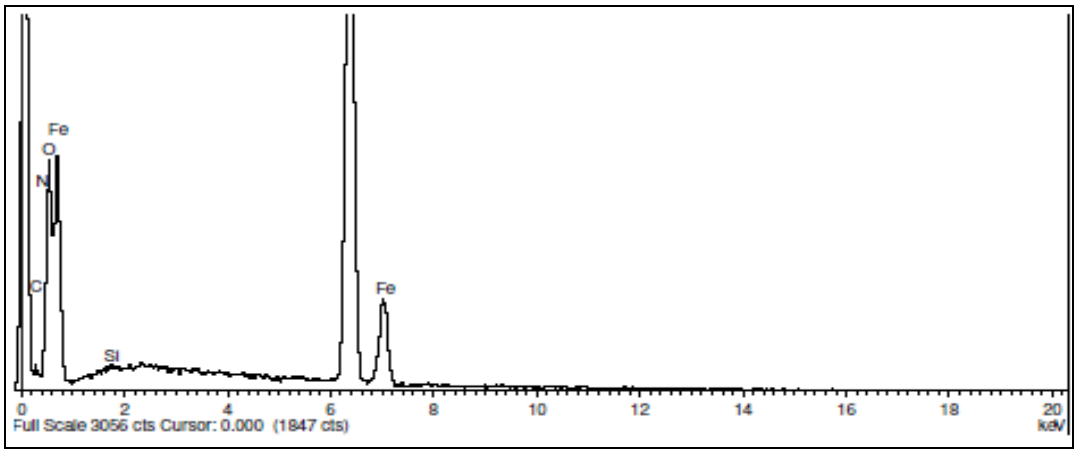

a. EDS for Blank (1M H_2SO_4)

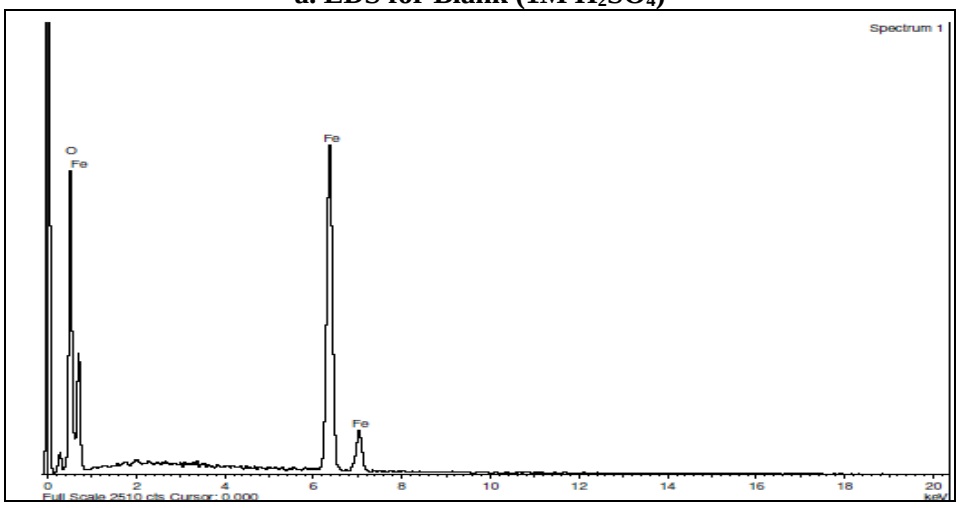

EDS for PE-FG + 1M H_2SO_4

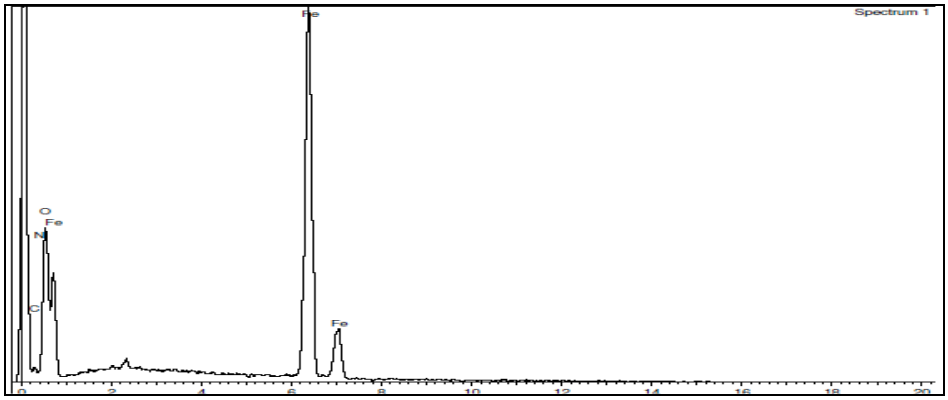

Figure 5 EDS image of PE-FG and mild steel after 3 hours of immersion in 1M H_2SO_4 without and with inhibitor

Table 1 Surface compositions (weight %) of polyester composite and mild steel after 3 hours of immersion in 1M H_2SO_4 without and with inhibitor

Name	% Mass				
	Fe	C	N	O	Si
PE-FG	65.10	6.57	4.74	23.49	0.10
Blank	66.20	-	-	33.80	-
PE-FG	60.59	5.93	5.39	28.09	-

Weight loss measurements

As shown in **Figure 6** and **Table 2**, pure PE and PE-FG composites were exposed to mild steel corrosion in 1M H2SO4 media. When PE is used at 500ppm, the inhibition effectiveness is only 38.6%, but with the composite (PE-FG), the inhibition efficiency improves up to 90% when the concentration of filler is increased (FG). A good anticorrosion characteristic can be deduced from the results, which shows that the corrosive rate reduces with increasing weight of FG in polyester composite (100ppm, 300ppm and 500ppm) [26].

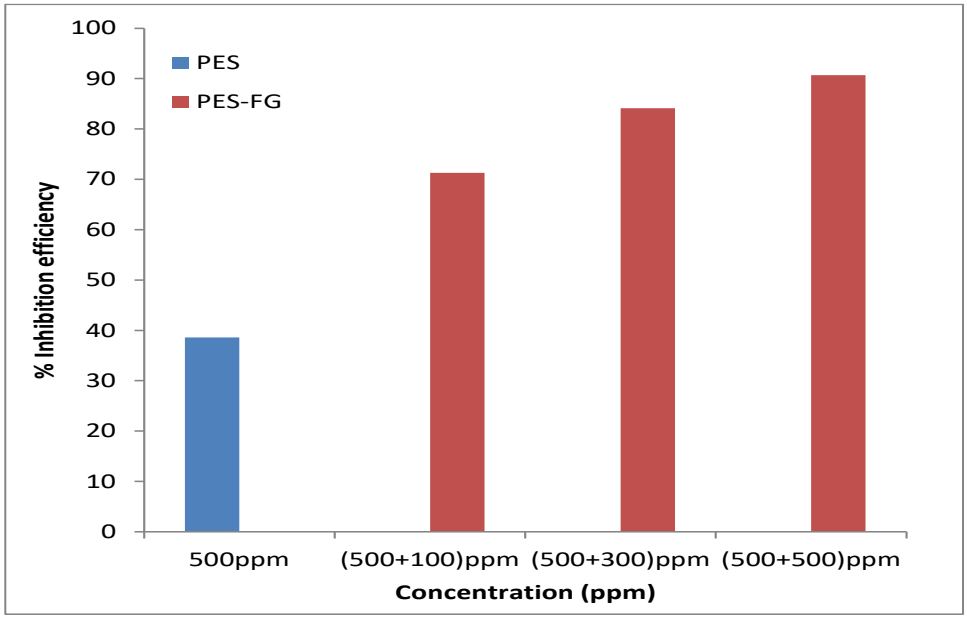

Figure 6 Plot of inhibition efficiency (%) Vs concentration (ppm) for the inhibition of corrosion of mild steel in 1M H_2SO_4

Table 2 Inhibition efficiencies at polyester / polyester composite for corrosion of mild steel in 1M H_2SO_4 from weight loss measurement at 303±1K

Name of the inhibitors	Conc. of PE (ppm)	Weight of filler material (ppm)	Weight loss (g)	Inhibition efficiency (%)	Degree of surface coverage (Θ)	Corrosion rate ($gcm^{-2}h^{-1}$)
Blank	-	-	0.2209	-	-	14.31
PE	500	-	0.1356	38.6	0.3862	8.78
FG	-	500	0.0724	67.23	0.6723	4.69
PE-FG	500	FG - 100	0.0634	71.29	0.7129	4.11
		FG - 300	0.0351	84.11	0.8411	2.27
		FG - 500	0.0206	90.67	0.9067	1.33

Effect of temperature

Weight loss studies were done at 303K - 333K to establish the inhibition mechanism and kinetic characteristics of the corrosion process. It's shown in **Table 3** how temperature affects mild steel's corrosion resistance, both in the absence and presence of the composite. Corrosion rates increase and inhibition efficiency diminishes as the temperature rises. Adsorption of additives on metal surfaces is demonstrated by such behaviour. Corrosion rate (CR) of mild steel in acidic media and temperature exhibit Arrhenius-type relationship in **Figure 7** shows the plot of log CR vs 1/T. Polyester and polyester composite have activation energies of 46.22 and 54.01 kJ/mol, respectively (**Table 4**). Considering that these values are greater than the value of 37.36 kJ/mol obtained for the blank, this indicates that the

polyester composite retards the corrosion response of mild steel It also supports the physical adsorption phenomena [31].

Table 3 Inhibition efficiencies of polyester / polyester composite for corrosion of mild steel in 1M H_2SO_4 from weight loss measurement at higher temperature

Name of the inhibitors	Temperature (K)	Weight loss (g)	Inhibition efficiency (%)	Corrosion rate ($gcm^{-2}h^{-1}$)
Blank	303	0.0736	-	14.31
	313	0.1350	-	26.24
	323	0.1979	-	38.46
	333	0.2846	-	55.31
PE (500ppm)	303	0.0452	38.58	8.79
	313	0.0956	29.19	18.58
	323	0.1533	22.53	29.80
	333	0.2410	15.11	46.96
PE-FG (500ppm +500ppm)	303	0.0068	90.76	1.32
	313	0.0183	86.44	3.56
	323	0.0304	84.63	5.91
	333	0.0486	82.92	9.45

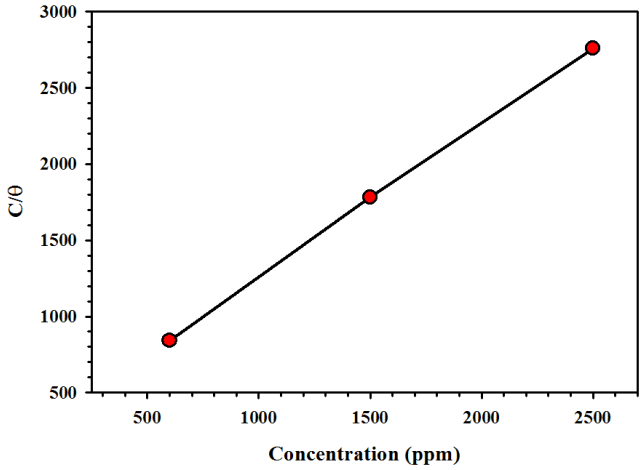

Figure 7 Arrhenius plot of corrosion of mild steel in 1M H_2SO_4 solution in the absence and presence of inhibitors

Table 4 Activation parameters of mild steel corrosion in 1M H_2SO_4 for polyester / polyester composite calculated by Arrhenius, transition state thermodynamic equations

Name of the inhibitors	E_a (kJ/mol)	ΔG°_{ads} (kJ/mol)				ΔH° (kJ/mol)	$-\Delta S^{\circ}$ (kJ/mol/K)
		303 K	313 K	323 K	333 K		
Blank	37.36	67.42	68.50	69.58	70.65	34.72	0.1079
PE (500ppm)	46.22	68.61	69.44	70.27	71.09	43.58	0.0826
PE-FG (500ppm+ 500ppm)	54.01	73.24	73.96	74.68	75.40	51.37	0.0722

Determination of the activation complex's activation enthalpy (ΔH°) and entropy (ΔS°). **Figure 8** shows the plot of log corrosion rate/T vs 1/T. ΔH° /2.303R) and ΔS° /2.303R) are the slope and intercept of the straight lines, respectively [32]. In Table 4, the values of ΔH° and ΔS° are computed using these two variables, respectively. Due to the endothermic nature of mild steel dissolution, positive ΔH° values indicate that mild steel dissolution is problematic in the presence of inhibitors [33]. For mild steel dissolving, in 1M H_2SO_4 with inhibitors, the ΔH° values (43.58 and 51.37 kJ/mol) are greater than in the absence of inhibitor (34.72 kj/mol), suggesting higher protection efficiency. Table 4 shows this. When inhibitors are present, the values of ΔS° (Table 4) tend to be less negative than they would be in the absence of any inhibitors. Table 4 shows that the entropy of activation ΔS° increased in the presence of the inhibitors relative to the free acid solution. Surfaces coated with inhibitor molecules prevent hydrogen ions from discharging at the metal surface, increasing disorder [34]. Table 4 shows the ΔG° values. When inhibitors are added to inhibited systems, the activated corrosion complex becomes less stable relative to its absence, as seen by ΔG° values.

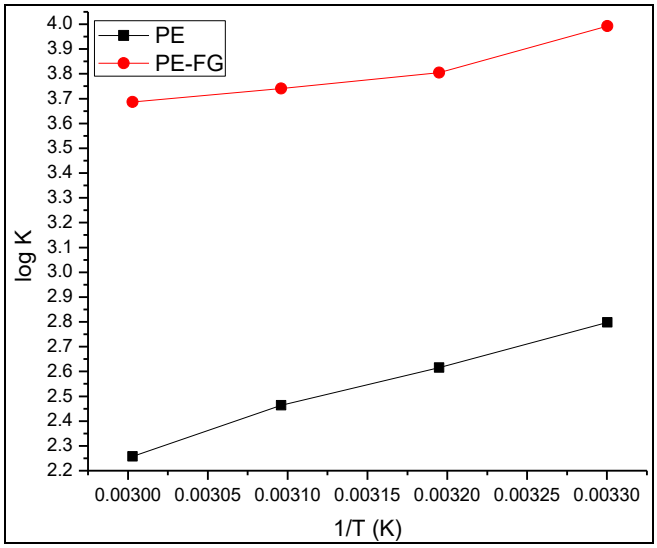

Figure 8 Transition plot of corrosion of mild steel in 1M H_2SO_4 solution in the absence and presence of inhibitor

Adsorption isotherm and Thermodynamic parameters

The adsorption (PE and PE-FG) isotherm provides basic information on the interaction between the inhibitor and the mild steel surface. Langmuir, Temkin, Frumkin and Flory-Huggins was used to try to match the data to various isotherms. The Langmuir isotherm provided the best fit. At 303K, **Figure 9** illustrates the plot of C/θ versus C. We found that the adsorbed inhibitor molecules form monolayers on the mild steel surface, and that there is no contact between the adsorbed inhibitor molecules [36] Adsorption free energy ($\Delta G°_{ads}$) values are provided in **Table 5**. On average, our observations showed values between 25.52 to 34.63 KJ/mol for $\Delta G°_{ads}$ (Kilojoules per Mole). Accordingly, the inhibitors adsorbing to the surface of mild steel in 1M H_2SO_4 are the result of a physical process [37, 38]. On mild steel surfaces, the inhibitor is electrostatically adsorbed to create an insoluble and persistent inhibitor coating, which reduces metal dissolution. Nitrogen and oxygen molecules with a lone pair of electrons and aromatic rings with electrons accelerate this process. As shown in **Figure 10**, the slope of log K_{ads} is equal to - $\Delta H°/2.303R$ and the intercept is equal to - $\Delta S°/2.303R$ + log1/55.5 [39]. Calculated values of $\Delta H°_{ads}$ (Enthalpy of Adsorption) and $\Delta S°_{ads}$ (Entropy of Adsorption) for Thermodynamic Parameters are shown in **Table 6**. Variation of $\Delta G°/T$ with respect to $\Delta G°$ /T yields a straight line with slope equal to $\Delta H°/T$ in **Figure 11**. According to the graph in **Figure 12**, there is no slope or intercept for the relationship between $\Delta G°_{ads}$ and T. Instead, the slope and intercept are both equal to $-\Delta S°_{ads}$. Adsorption of polyester and its compound is an exothermic reaction, as indicated by the negative sign on $\Delta H°_{ads}$. According to the current example, $\Delta H°$ is bound at a rate of 40 $kJmol^{-1}$, which confirms the presence of physical adsorption [40-42].

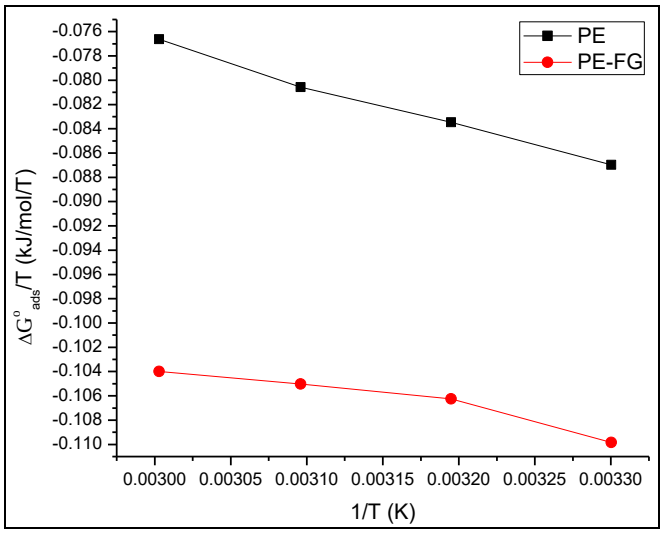

Figure 9 Langmuir plot of inhibitor in 1M H_2SO_4 Fig. 10 The relationship between $\Delta G^{\circ}_{ads}/T$ and 1/T

Table 5 Free energy of adsorption of mild steel corrosion in the presence of polyester / polyester composite in 1M H_2SO_4

Name of the inhibitors	$-\Delta G^{\circ}_{ads}$(kJ/mol)			
	303 K	313 K	323 K	333 K
PE (500ppm)	26.35	26.13	26.03	25.52
PE-FG (500ppm+500ppm)	33.28	33.25	33.92	34.63

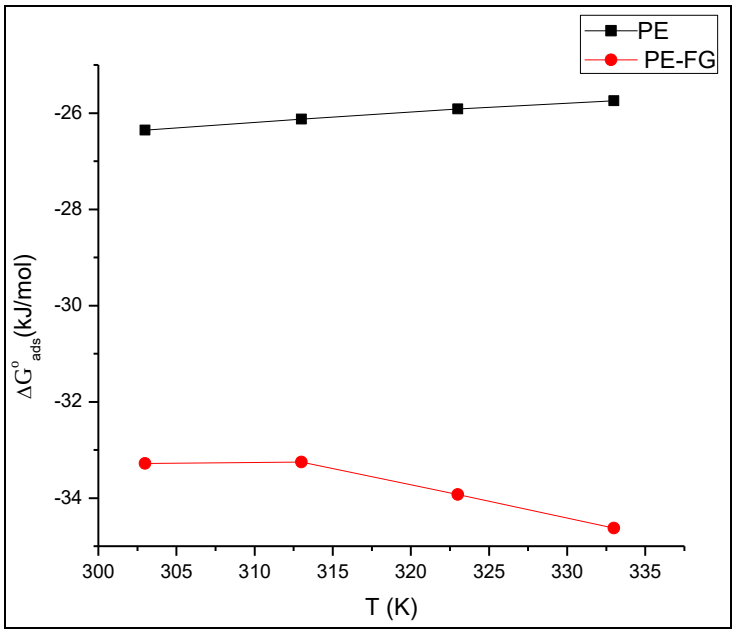

Figure 10 The relationship between $\Delta G^{\circ}_{ads}/T$ and 1/T

Table 6 Heat of adsorption and entropy of adsorption values calculated by different thermodynamic equations

Name of the inhibitors	Van't Hoff equation		Gibbs Helmholtz equation	Basic thermodynamic equation	
	$-\Delta H^0$ kJ/mol	$-\Delta S^0$ kJ/mol/K	$-\Delta H^0$ kJ/mol	$-\Delta H^0$ kJ/mol	$-\Delta S^0$ kJ/mol/K
PE (500ppm)	34.21	0.0258	34.21	34.32	0.0262
PE-FG (500ppm + 500ppm)	19.11	-0.0461	19.11	18.82	-0.0470

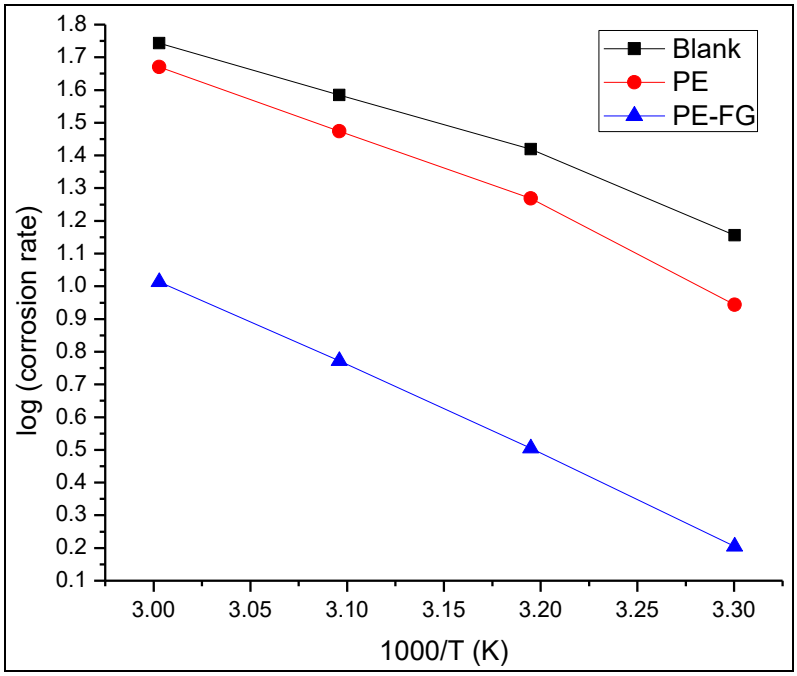

Figure 11 The relationship between ΔG°_{ads} and T

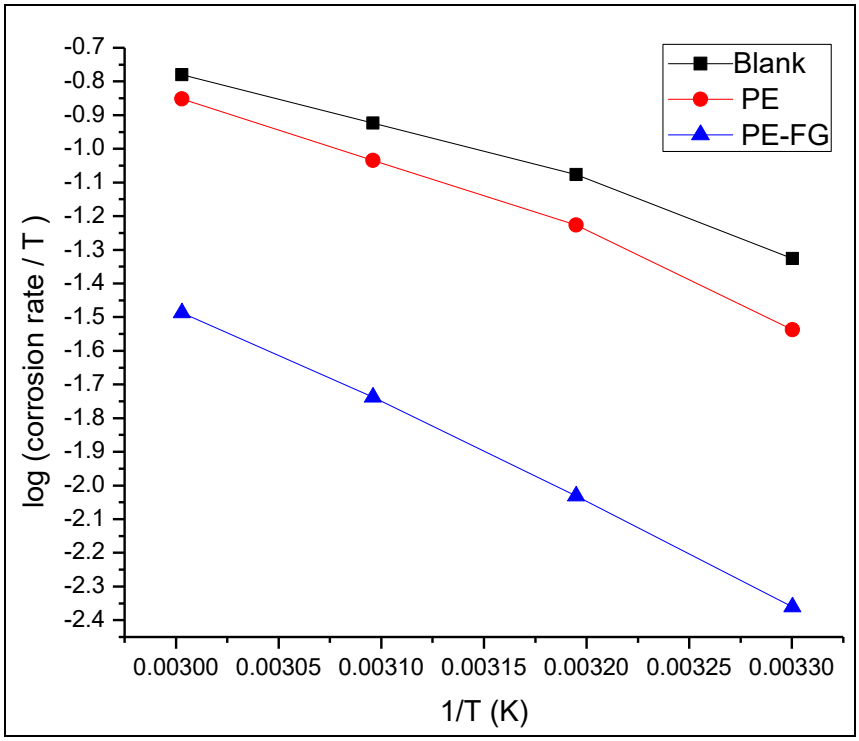

Figure 12 The relationship between log K_{ads} and 1/T

Electrochemical Measurements: Polarization studies

The potentiodynamic polarization behavior of mild steel in 1M H_2SO_4 containing PE (500ppm) and PE-FG (500ppm PE + 100ppm / 300ppm / 500ppm of FG) is shown in **Figure 13** and the corrosion parameters calculated are tabulated in **Table 7**. Both the anodic and cathodic current potential curves are extrapolated in order to derive corrosion potential (E_{corr}) and corrosion current density (I_{corr}) from their interaction [38-42]. Analysis of this table's data reveals a decrease in both cathodic and anodic currents as FG concentration increases, with no discernible movement in E_{corr} values. It may be deduced from such an observation that the inhibitors are of mixed kind, with PE being somewhat more anodic and PE-FG composite slightly more cathodic.

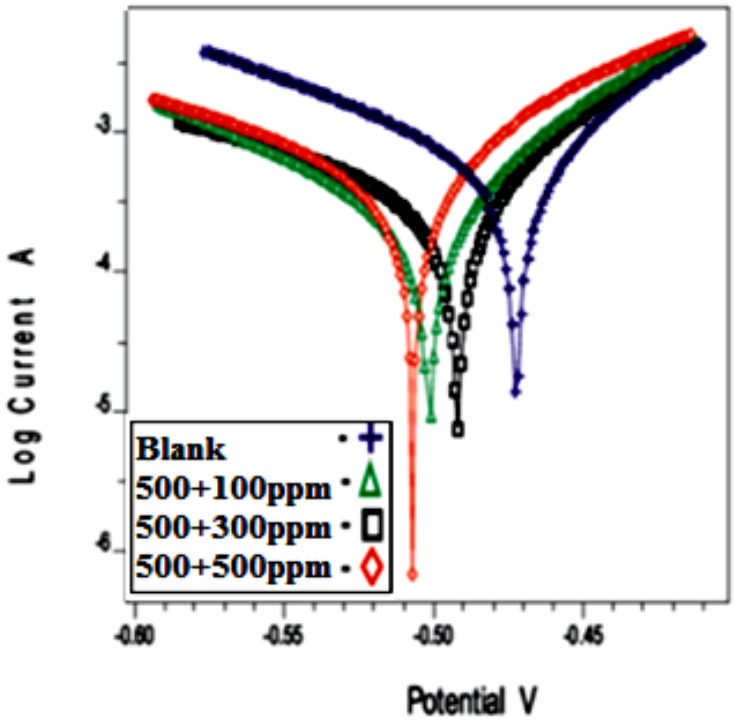

Figure 13 Polarization curves for mild steel recorded in 1M H_2SO_4 for selected concentrations of the inhibitor PE-FG

Table 7 Corrosion parameters of polyester / polyester composite for corrosion of mild steel in 1M H_2SO_4 by potentiodynamic polarization method

Name of the inhibitors	Conc. of PE	Weight of filler material	Tafel slopes (mV/dec)		E_{corr} (mV)	I_{corr} (μAmp/cm^2)	Inhibition efficiency (%)
			b_a	b_c			
Blank	-	-	52	112	-467.4	1569	-
PE	500ppm	-	34	177	-451.3	990	36.9
PE-FG	500ppm	FG- 100ppm	80	111	-503.4	932	40.6
		FG- 300ppm	57	133	-490.9	772	50.8
		FG- 500ppm	84	115	-513.8	468	70.1

Electrochemical impedance spectroscopy

EIS at 303K examined the corrosion behaviour of mild steel in acidic solution in the presence of PE and PE-FG. Mild steel in uncontrolled and inhibited acidic solutions with varied concentrations of PE-FG is shown in **Figure 14** with a capacitive arc and the resulting impedance values in **Table 8**. Charge transfer resistance R_{ct} increases and double layer capacitance C_{dl} decreases with increasing inhibitor concentration, as shown in the table. The increase in the thickness of the electrical double layer is the cause of the decrease in C_{dl}. Inhibitor molecule adsorption at the metal solution interface might explain this phenomenon.

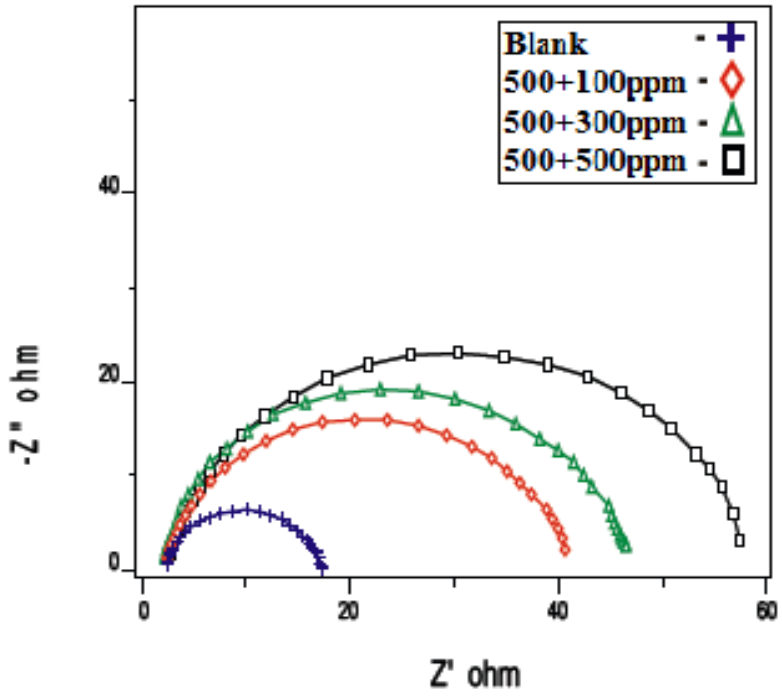

Figure 14 Nyquist diagram for mild steel in 1M H_2SO_4 for selected concentrations of Inhibitor PE-FG

Table 8 AC-impedance parameters for corrosion of mild steel at the inhibitor concentration of polyester / polyester composite in 1M H_2SO_4

Name of the inhibitors	Concentration of PES	Weight of filler material	R_{ct} (ohm cm^2)	C_{dl} (μF/cm^2)	Inhibition efficiency (%)
Blank	-	-	11.06	27.8	-
PE	500ppm	-	20.8	25.2	46.83
PE-FG	500ppm	FG- 100ppm	36.0	23.1	69.28
		FG- 300ppm	43.66	22.6	74.66
		FG- 500ppm	53.08	16.3	79.16

Atomic Absorption Spectrophotometric Studies (AAS)

As a result of the AAS data, the inhibitory efficiency (percent) of polymer and polymer composite was computed, and the results are shown in **Table 9**. There was a good agreement between the inhibitory efficiency (percent) of this approach and that achieved from conventional weight reduction methods.

Table 9 Amount of dissolved iron present in the corrosive solution with and without inhibitors in 1M H_2SO_4 measured using atomic absorption spectrometer

Name of the inhibitors	Concentration of PES	Weight of filler materials	Amount of iron content (mg/l)	Inhibition efficiency (%)
Blank	-	-	1304.96	-
PES	500ppm	-	829.22	36.5
PES-RH	500ppm	FG- 100ppm	388.42	70.24
		FG- 300ppm	202.30	84.50
		FG- 500ppm	156.64	88.12

Mechanism of inhibition

It is generally accepted that the first stage in the action mechanism of organic compounds in an aggressive acidic media is their adsorption onto a metal-solution interface. Water and oxygen are believed to be prevented from reaching the substrate surface by the polymer composite (well distributed functional graphene). This results in good corrosion prevention properties.

Conclusions

- The PES-FG composite as corrosion inhibitors were prepared by mixing of FG and PE through ultrasonication.
- PE showed only 38.6% inhibition efficiency at 500ppm while filler material FG, alone showed inhibition efficiency of 67% at a concentration of 500ppm. But in the case of composite the inhibition efficiency increased upto 90%, with increasing concentration of the filler FG up to 500ppm.
- EIS experiments demonstrated that as the concentration of inhibitor increases, the R_{ct} increases and C_{dl} decreases, owing to the increased thickness of the adsorbed layer.
- The Tafel slopes obtained from potentiodynamic polarization curves indicated that all the inhibitors behaved as mixed type.
- The FT-IR, SEM, EDS and powder XRD reveal the formation of protective layer on the mild steel surface.

Reference

[1] Vinothkumar K, Nivetha M, Sethuraman MG (2020) Robust composite coating with superior corrosion inhibitory performance on surgical grade 316L stainless steel in Ringer solution. Iran Polym J 29:919–931

[2] Hamidi Z, Mosavian SY, Sabbaghi N (2020) Cross-linked poly(N-alkyl-4-vinylpyridinium) iodides as new eco-friendly inhibitors for corrosion study of St-37 steel in 1 M H2SO4. Iran Polym J 29:225–239

[3] Pekdemir ME, Öner E, Kök M (2021) Thermal behavior and shape memory properties of PCL blends film with PVC and PMMA polymers. Iran Polym J 30: 633–641

[4] Dagdag O, El Harfi A, El Gana L, Hlimi Z, Erramli H, Hamed O, Jodeh S (2019) The role of zinc phosphate pigment in the anticorrosion properties of bisphenol a diglycidyl ether-polyaminoamide coating for aluminum alloy AA2024-T3. J Bio-Tribo-Corros 5(1):7-16

[5] Huang R, Guo X, Ma S, Xie J, Xu J, Ma J (2020) Novel phosphorus-nitrogen-containing ionic liquid modified metal-organic framework as an effective flame retardant for epoxy resin. Polymers 12(1):108-120

[6] Dagdag O, Hsissou R, Berisha A, Erramli H, Hamed O, Jodeh S, El Harfi A (2019) Polymeric-based epoxy cured with a polyaminoamide as an anticorrosive coating for aluminum 2024–T3 surface: experimental studies supported by computational modeling. J Bio-Tribo-Corros 5:58-64

[7] Levchik GF, Grigoriev YV, Balabanovich AI, Levchik SV, Klatt M (2000) Phosphorus-nitrogen containing fire retardants for poly (butylene terephthalate). Polym Int 49:1095–1100

[8] Jadhav SA, Rane A, Abitha V, Suchithra P, Patil SS, Narute ST (2015) Polymeric particle board: a sustainable substitute to wooden boards. Moroc J Chem 3:2723–2729

[9] Dagdag O, El Bachiri A, Hamed O, Haldhar R, Verma C, Ebenso E, El Gouri M (2021) Dendrimeric epoxy resins based on hexachlorocyclotriphosphazene as a reactive flame retardantpolymeric materials: a review. J Inorg Organomet Polym Mater 3:1–22

[10] Dagdag O, Berisha A, Safi Z, Hamed O, Jodeh S, Verma C, Ebenso E, El Harfi A (2020) DGEBA-polyaminoamide as effective anti-corrosive material for 15CDV6 steel in NaCl medium: computational and experimental studies. J Appl Polym Sci 137:48402-48410

[11] Dagdag O, Essamri A, El Gana L, El Bouchti M, Hamed O, Cherkaoui O, Jodeh S, El Harfi A (2019) Synthesis, characterization and rheological properties of epoxy monomers derived from bifunctional aromatic amines. Polym Bull 76:4399–4413
[12] Dagdag O, El Gana L, Hamed O, Jodeh S, El Harfi A (2019) Anticorrosive formulation based of the epoxy resin-polyaminoamide containing zinc phosphate inhibitive pigment applied on sulfo-tartaric anodized AA 7075–T6 in NaCl medium. J Bio-Tribo-Corros 5:25-32
[13] Bekhta A, Elharfi A (2016) Comparative study of the rheological and thermal properties of the formol phenol novolac epoxy and those of the model resin diglycidylether of bisphenol A (DGEBA). Moroccan J Chem 4:61–67
[14] Li L, Cai Z (2020) Flame-retardant performance of transparent and tensile-strength-enhanced epoxy resins. Polymers 12:317-324
[15] Song K, Wang Y, Ruan F, Liu J, Li N, Li X (2020) Effects of a macromolecule spirocyclic inflatable flame retardant on the thermal and flame retardant properties of epoxy resin. Polymers 12:132-140
[16] Rane AV, Abitha V, Jadhava S (2020) Non-isocyanate polyurethane systems: a review. Moroc J Chem 8:8–4
[17] Amin MA, Abd El-Rehim SS, El-Sherbini EEF, Bayoumi RS (2007) The Inhibition of low carbon steel corrosion in hydrochloric acid solutions by succinic acid: Part I. Weight loss, polarization, EIS, PZC, EDX and SEM studies. Electrochim Acta 52: 3588-3600
[18] Kanojia R, Singh G (2005) An interesting and efficient organic corrosion inhibitor for mild steel in acidic medium. Surface Eng 21(3):180–186
[19] Ferry M, Mohd Noor CW, Gaspersz F, Manuputty (2013) Corrosion performance of mild steel in seawater inhibited by allium CEPA. J.Eng Compute Appl Sci 2: 3-8
[20] Lalitha A, Ramesh S, Rajeswari S (2005) Surface protection of copper in acid medium by azoles and surfactants. Electrochim Acta 51:47-55
[21] Srikanth AP, Sunitha TG, Raman V, Nanjundan S, Rajendran N (2007) Synthesis, characterization and corrosion protection properties of poly(N-(acryloyloxymethyl) benzotriazole-co-glycidyl methacrylate) coatings on mild steel. Mater Chem Phys 103: 241-247
[22] Li W, He Q, Zhang S, Pei C, Hou BJ (2008) Some new triazole derivatives as inhibitors for mild steel corrosion in acidic medium. Appl Electrochem 38:289-295
[23] Sivakumar PR, Srikanth AP (2016) Anticorrosive activity of Santalum Album leaves extract against the corrosion of mild steel in acidic medium. Int J Phy Appli Sci 3 (1):10-20
[24] Sivakumar PR, Karuppusamy M, Perumal S, Elangovan A, Srikanth AP (2015) Corrosion Inhibitive effects of Madhuca Longifolia on mild steel in 1N HCl solution. J Envi Nanotech 4(2):31-36
[25] Karuppusamy M, Sivakumar PR, Perumal S, Elangovan A, Srikanth AP (2015) Mimusops Elengi Linn plant extract as an efficient green corrosion inhibitor for mild steel in acidic environment. J Envi Nanotech 4(2):09-15
[26] Sivakumar PR, Karuppusamy M, Vishalakshi K, Srikanth AP (2016) The inhibition of mild steel corrosion in 1N HCl solution by Melia Azedarach leaves extract. Der Pharma Chem 8(12): 74-83.
[27] Sivakumar PR, Srikanth AP (2016) Inhibiting effect of seeds extract of Pithecellobium Dulce on corrosion of mild steel in 1N HCl medium. Int J Eng Sci and Comp 6(8): 2744-2748
[28] Sivakumar PR, Karuppusamy M, Vishalakshi K, Srikanth AP (2016) The inhibition of mild steel corrosion in 1N HCl solution by Melia Azedarach leaves extract. Der Pharma Chemi 8(12):74-83.
[29] Sivakumar PR, Vishalakshi K, Srikanth AP (2016) Inhibitive action of Bombax Malabricum leaves extract on the corrosion of mild steel in 1N HCl Medium. J Appli Chemi 5(5):1080-1088
[30] Vishalakshi K, Sivakumar PR, Srikanth AP (2016) Tetrameles Nudiflora Leaves Extract as Green Corrosion Inhibitor for Mild steel in Hydrochloric Acid Solution. Int Org Sci Res J Appl Chemi 9(9):50-55
[31] Sivakumar PR Srikanth AP (2016) Inhibiting effect of fruits extract of Santalum Album on corrosion of mild steel in Hydrochloric acid solution. Int Org Sci Res J Appl Chemis 369(10): 29-37
[32] Sivakumar PR, Srikanth AP (2016) Inhibitive action of aqueous extract of Holoptelea integrifolia leaves for the corrosion of mild steel in 1N HCl solution. Der Phar Chemi 8(19):433-440
[33] Sivakumar PR, Karuppusamy M, Vishalakshi K, Srikanth AP (2017) Inhibitory effect of Michelia Champaca leaves extracts on the corrosion of mild steel in 1N HCl acid: A Green Approach. IOSRD Int J Chemi 4(1):14-18
[34] Sivakumar PR, Srikanth AP (2017) Anticorrosive Activity of Schereabera sweietenoids Leaves as Green Inhibitor for Mild Steel in Acidic Solution. Asian J Chemi 29(2):274-278
[35] Vishalakshi K, Sivakumar PR, Srikanth AP (2016) Analysis of Corrosion Resistance behavior of green inhibitors on mild steel in 1N HCl medium using electrochemical techniques. Der Pharma Chemica, 8(19),

548-553
[36] Sivakumar PR, Srikanth AP (2017) Ziziphus jujube leaves extract as green corrosion inhibitor for mild steel in 1N hydrochloric acid Medium. J Appli Chemis 6(4):476-483
[37] Sivakumar PR, Srikanth AP (2018) Eco friendly green inhibitor for corrosion of mild steel in 1N hydrochloric acid Medium. J Appli Chemis 7(1):239-249
[38] Sivakumar PR, Srikanth AP (2018) Gloriosa superba linn extract as eco friendly inhibitor for mild steel in acid medium: A comparative study. Asi J Chemis 30(3):513-519
[39] Sivakumar PR, Srikanth AP, Muthumanikam S (2017) The corrosion inhibition and adsorption properties of ecofriendly green inhibitor - A comparative study. Int J Chemtech Res 10(12):386-398
[40] Sivakumar PR, Karuppusamy M, Srikanth AP (2017) Corrosion inhibition of mild steel in 1N HCl media using Millingtonia Hortensis leaves extract. Int Org Sci Res J Appl Chemi 10:65-70
[41] Sivakumar PR, Karuppusamy M, Srikanth AP (2018) Pithecellobium dulce extracts as corrosion inhibitor for mild steel in acid medium. Der Pharma Chemi 10:22-28
[42] Sivakumar PR and Srikanth AP (2020) Green corrosion inhibitor: A comparative study. Sadhana 45:45-56
[43] Devarayan Kesavan, Mayakrishnan Gopiraman, Nagarajan Sulochana Green inhibitors for corrosion of metals: a review, Chemical Science Review and Letters, 2012,1,1-8
[44] Sukumaran, M., Devarayan, K., & Marimuthu, R. (2021). Eco-friendly inhibitor for corrosion of TMT rod in marine environment. Materials Today: Proceedings. Article in press. DOI:10.1016/J.MATPR.2021.11.460
[45] Velayutham Rajeswari, Kesavan Devarayan, Periasamy Viswanathamurthi Expried pharamaceutical inhibitor for cast iron corrosion in acidic medium, Research on Chemical intermediates, 43(7), 2017, 3893-3913.
[46] M. A. Tigori, A. Kouyate, V. Kouakou, P. M. Niamien and A. Trokourey, Quantum chemical study of some antihistamines as inhibitor corrosion for copper in nitric acid solution using DFT method, Chemical Science Review and Letters, https://doi.org/10.37273/chesci.cs2051018
[47] Busayo A. Tomilawo, Emmanuel F. Olasehinde, Julius U. Ani, Fredrick O. Obagboye, Jonnie N. Asegbeloyin, Innocent O. Obi, Linus E. Aneke,Corrosion control of mild steel in sulphuric acid by Athyrium filix-femina leaf extraxt green inhibitors Chemical Science Review and Letters, doi.:10.37273/chesci.cs0320510701
[48] Kavitha Rose, Monikandon Sukumaran, Kesavan Devarayan, and Sankar Arumugam Evidence for homogeneous adsorption of samanea saman extract inhibitor on steel surface international journal of chemical science 15.2(2017)
[49] Kavitha Rose, Monikandon Sukumaran, Kesavan Devarayan, Kalyanaraman Rajagopal, Sankar Arumugam, Inhibition of steel corrosion in acid medium by ethanolic extract of cassia fistula, Chem Sci Rev Lett 2016, 5(20), 59-66.
[50] Kavitha Rose, Byoung-Suhk Kim, Kalyanaraman Rajagopal, Sankar Arumugam, Kesavan Devarayan, Surface protection of steel in acid medium by Tabernaemontana divaricate extract: physicochemical evidence for adsorption of inhibitor, journal of molecular Liquids, 2016, 214:111-116.

Publication History
Received 30.10.2021
Revised 04.02.2022
Accepted 06.02.2022
Online 31.03.2022